

Special issue article

# Early changes in the synapses of the neostriatum induced by perinatal asphyxia

M. Grimaldi<sup>1</sup>, I. Romer<sup>1</sup>, M. T. González de Apodaca<sup>1</sup>, L. Iturbe<sup>1</sup>, I. D. Catania<sup>1</sup>, J. González<sup>3</sup>, R. Kolliker-Fres<sup>1</sup>, G. Barreto<sup>3</sup>, F. Capani<sup>1,2</sup>

<sup>1</sup>Universidad Argentina John F Kennedy, Buenos Aires, Argentina, <sup>2</sup>Instituto de Investigaciones Cardiológicas Prof Dr Alberto Taquini, Buenos Aires, Argentina, <sup>3</sup>Facultad de Ciencias, Departamento de Nutrición y Bioquímica, Pontificia Universidad Javeriana, Bogotá D.C., Colombia

Perinatal asphyxia (PA) is a medical condition associated with a high short-term morbimortality and different long-term neurological diseases. In previous work we have observed at 6 months post-synaptic densities (PSDs) alterations compatible with neurodegeneration highly correlated with the increment in the ubiquitination. Although alterations in the synaptic organization and function have been related with neuronal death after hypoxia, little is known about the synaptic changes in young animals exposed to PA. The main aim of this work is to study the PSDs changes in striatum of 30-day-old rats subjected to PA. Using two-dimensional electron microscopic analyses of synapses staining with ethanolic phosphotungstic acid we observed an increment of PSD thickness in severe hypoxic rats. These data are consistent with the western blot analysis that showed an increment in ubiquitination levels in the synapses of severe hypoxic rat. We did observe any alterations neither in synaptic structure nor in ubiquitination in mild asphyctic rats. These data suggest that hypoxia might cause early misfolding and aggregation of synaptic proteins in severe anoxic animals that could induce long-term neurodegeneration.

**Keywords:** Neostriatum, Post-synaptic density, Rat, Synapse, Ubiquitination

## Introduction

Perinatal asphyxia (PA) is an important cause of short- and long-term neurological diseases.<sup>1</sup> The vulnerable areas of the central nervous system to the hypoxic–ischemic insult are primarily localized in the hippocampus, cerebral cortex, and basal ganglia.<sup>2,3</sup> Following PA, approximately 45% of newborns die and 25% have permanent neurological deficits including cerebral palsy, mental retardation and developmental delay, learning disabilities, visual and hearing impairments, and different issues in the school readiness (Amiel-Tison *et al.*, 1986; Gunn *et al.*, 2000).<sup>4–7</sup>

Previous works have shown<sup>8–11</sup> that the most important causes for neuronal damage and death in striatum and necrotic during ischemic–hypoxic process are related with a chain of events that include the over production of excitatory amino acids, nitric oxide, and finally the increased release of reactive oxygen species (ROS). Although the immature brain is relatively protected from hypoxia by adaptive mechanisms, severe insults can trigger self-sustaining

damaging cascades lasting for days or weeks resulting in prominent injury.<sup>12–15</sup>

Cells degrade misfolded proteins through the ubiquitin-proteasome system (UPS). Under pathological conditions, protein misfolding causes exposure of hydrophobic segments, becoming them aggregated.<sup>16</sup> Although dysfunction of UPS and protein aggregation has been related with the neuronal death after ischemia,<sup>16–18</sup> the mechanisms of cerebral hypoxia damage are not still completely understood.

We have previously described long-term alterations in neuronal and synaptic level in rat neostriatum after hypoxia<sup>9,13,19</sup> that are well correlated with behavioral changes.<sup>20,21</sup> However, it is not clear whether the synaptic striatal alterations are present in young PA animals. Therefore, in the present study, we combined electron microscopy techniques and ethanolic phosphotungstic acid (E-PTA) staining to study the post-synaptic densities (PSDs) alterations in neostriatum after 1 month of the birth-PA induction when synapses are well established.<sup>22</sup> We also provide evidence that ubiquitin protein conjugates are deposited in PSDs of severe PA animals. Furthermore, our data suggest that the persistent PSDs ubi-protein formation might

Correspondence to: F. Capani, Instituto de Investigaciones Cardiológicas, Universidad Argentina John F Kennedy, Buenos Aires, Argentina. Email: franciscocapani@hotmail.com

be one of the mechanisms that can induce delayed neuronal damage during the post-hypoxic phase. Therefore, we hypothesize that the early changes in the PSDs of the rat neostriatum could be the beginning point of the events that produce the important modification and ubiquitination observed in the PSDs in asphyctic adult rats.

## Materials and methods

### Experimental animals

All animal experimental procedures and care were approved by the Ethical Board of School of Medicine, University of Buenos Aires, Argentina. In the present study were used 15 full pregnant Sprague Dawley rats. Pregnant rats were placed in the separate cages at Day 14 of their gestation and maintained in a temperature-controlled environment on a 12-hour light/dark cycle and fed with Purina chow and tap water *ad libitum*. A group were used as surrogate mothers ( $n = 5$ ) and the rest to perform the PA experiments ( $n = 10$ ).

### Induction of asphyxia

Full-term pregnant rats were rendered unconscious by CO<sub>2</sub> inhalation,<sup>23</sup> rapidly decapitated, and immediately hysterectomized after their first pup delivered vaginally (vaginal control) (Bjelke *et al.*, 1991).<sup>24</sup> One uterine horn, containing the fetuses, was placed in a water bath at 37°C for 10 and 15 minutes (mild PA); 19 minutes (severe PA). Following asphyxia, the uterus horn was rapidly opened; the removed pups were stimulated to breathe by cleaning up the amniotic fluid and by performing tactile intermittent stimulation with pieces of medical wipes for few minutes until regular breathing can be established. The umbilical cord was ligated and the animals were left to recover for 1 hour under a heating lamp. When their physiological conditions improved, they were given to surrogate mothers who had delivered normally within the 24 hours before the experiments. The different groups of pups were marked and mixed with surrogate's normal litters. We maintained litters of eight pups with each surrogate mother. (For more details of this procedure see Capani *et al.*<sup>13,19</sup>.)

### Post-asphyxia procedures

One-month-old male rats ( $N = 3-5$  animals/group), were anesthetized with 28% (w/v) chloral hydrate, 0.1 ml/100 g of body weight, and perfused intracardially with paraformaldehyde 4% in phosphate buffer 0.1 M, pH 7.4. Brains were dissected and post-fixed in the same solution during 2 hours, and then immersed overnight in phosphate buffer 0.1 M, pH 7.4 containing 5% of sucrose. Coronal brain sections containing the neostriatum (40 and 100  $\mu$ m thick) were cut on an Oxford Vibratome and then

recovered for electron microscopic studies. Some of these sections were stained with cresyl violet according to the procedures described by Capani *et al.*<sup>13,19</sup>

### Electron microscopic studies

Tissue sections from experimental and control animals were stained either by the conventional osmium–uranium–lead method or by 1% E-PTA. Briefly, coronal brain sections were cut at thickness of 200  $\mu$ m with a Vibratome through the level of neostriatum and post-fixed for 1 hour with 4% glutaraldehyde in 0.1 M cacodylate buffer pH 7.4. For conventional osmium–uranium–lead staining, sections were post-fixed for 2 hours in 1% osmium tetroxide in 0.1 M buffer cacodylate buffer, rinsed in distilled water, and stained with 1% aqueous uranyl acetate overnight. The sections were then dehydrated in an ascending series of ethanol to 100%, followed by dry acetone, and embedded in Durcupan ACM resin. Thin sections were counterstained with lead citrate before examination in the electron microscope. For E-PTA staining, sections were dehydrated in an ascending series of ethanol to 100% and stained for 1 hour with 1% PTA stained prepared by dissolving 0.1 g of PTA in 10 ml of 100% ethanol and adding four drops of 95% ethanol. Then, sections were embedded in Durcupan ACM resin.

### Quantitative analyses of thin section

Neostriatal specimens were selected for quantitative analyses based on the quality of E-PTA staining and the degree of ultrastructural preservation, as determined from conventionally stained material from the same animals. Samples were analyzed from controls ( $n = 4$ ) and for post-asphyctic animals at 10 minutes ( $n = 3$ ); 15 minutes ( $n = 3$ ); and 19 minutes ( $n = 4$ ). Tissue sections were cut at thickness of 100 nm and examined and photographed at 80 keV at a magnification of 8300 $\times$  with a Zeiss 109 electron microscope. For each animal, five micrographs were obtained from neostriatum. As described above, each negative was digitized into a PC computer. Using NIH Image 1.6 PSDs were first manually outlined, and then the maximal thickness, minimum thickness, length, and total area of each PSD were determined. All synapses in which the PSD, intracleft line, and pre-synaptic grid were clearly visible were chosen for analysis. The selection criterion resulted in the analysis of between 30 and 60 PSDs per animal for each neostriatum.

### Subcellular fractionation and preparation of PSDs

The crude synaptosomal fraction (P2) was prepared according to the method described previously by Hu and Wieloch,<sup>25</sup> Liu *et al.*,<sup>17</sup> and Capani *et al.*<sup>13</sup> Neostriatum tissue was pooled from four rats of each experimental group (approximately 1 g) and homogenized with a Dounce homogenizer (25 strokes) in 15 vol. of ice-cold homogenization buffer containing

15 mM Tris base-HCl pH 7.6, 1 mM DTT, 0.25 M sucrose, 1 mM MgCl<sub>2</sub>, 1.25 µg/ml pepstatin A, 10 µg/ml leupeptin, 2.5 µg/ml aprotinin, 0.5 mM PMSF, 2.5 mM EDTA, 1 mM EGTA, 0.1 M Na<sub>3</sub>VO<sub>4</sub>, 50 mM NaF, and 2 mM sodium pyrophosphate. The homogenates were centrifuged at 800 g at 4°C for 10 minutes, and the supernatants were centrifuged at 10 000 g at 4°C for 15 minutes to obtain P2. This P2 fraction was loaded onto a sucrose density gradient of 0.85 M/1.0 M/1.2 M and centrifuged at 82 500 g for 2 hours at 4°C. The light membrane fraction was obtained from the 0.85/1.0 sucrose interface, and the synaptosomal fraction was collected from the 1.0 M/1.2 M sucrose interface. After washing with 1% Triton X100, synaptosomal pellets were collected by centrifugation and then subjected to a second 1.0 M/1.5 M/2.0 M sucrose density gradient centrifugation at 201 000 g, 4°C for 2 hours. The isolated PSD fraction was obtained from the 1.5 M/2.0 M interface of the sucrose gradients. The PSD fraction was diluted with an equal volume of 1% Triton X-100/300 mM KCl solution, mixed for 5 minutes, and centrifuged at 275 000 g for 1 hour. The PSDs were suspended in a buffer containing 50 mM Tris/HCl, pH 7.4, 0.5 mM DTT, 100 mM KCl, 10 µg/ml leupeptin, 5 µg/ml pepstatin, 5 µg/ml aprotinin, 0.2 mM phenylmethylsulfonyl fluoride, and 0.2 mM sodium orthovanadate. Then PSDs were dissolved in 0.3% sodium dodecyl sulfate for biochemical analysis.

### Western blot

Western blot analysis was carried out on 8% sodium dodecyl sulfate polyacrylamide gel electrophoresis (SDS-PAGE) for remaining subcellular fractions.<sup>25</sup> Samples containing 20 µg of proteins from the control group and experimental groups were applied to each lane in a slab gel of SDS-PAGE. After electrophoresis, proteins were transferred to an immobilon-P membrane. The membranes were incubated with a primary antibody that recognizes free ubiquitin and ubi-proteins (Chemicon, 1:2000) overnight at 4°C. Mouse anti-actin monoclonal antibody (Chemicon International, Temécula, CA, USA) was used as an internal loading control at a dilution of 1:5000. The membranes were then incubated with horseradish peroxidase-conjugated anti-mouse secondary antibody for 45 minutes at RT. The blots were developed with an ECL detection method (Amersham). The films were scanned, and the optical densities of protein bands were quantified using Kodak 1D gel analysis software.

### Statistical analysis

The results were expressed as the means ± standard deviation (SD), unless otherwise noted. Group differences between the means of the IR calbindin

neurons, the area of the PSDs, the length of the PSDs, the minimum and maximum thickness of the PSDs, and the optical densities of the protein bands from western blot analysis were revealed by six one-way analysis of variances (ANOVAs). If the overall ANOVA was significant, comparisons between each one of the experimental groups (i.e. PA 10 minutes, PA 15 minutes, PA 19 minutes, and the control group) were carried out by two-tailed Dunnett's *post hoc* test. When the assumption of homogeneity of variances was rejected by Levene's test (this was the case for the optical densities from the western blot analysis), the overall ANOVA was followed by the multiple comparison Dunnett's T3 *post hoc* test. Differences with a probability of 5% or less were considered to be significant ( $P < 0.05$ ). All the statistical analysis was performed using the SPSS 13.0 for Windows statistical package (SPSS Inc., Chicago, IL, USA).

## Results

### Effect of the PA on neuronal survival in vivo

We analyze alterations in striatal cells in the different time of 1-month-old PA rat. Cresyl violet staining showed a nuclear condensation in 19 minutes PA animals (Fig. 1). To confirm the type of these cells we observed osmium-lead stained material at electron microscopic level. Clear nuclear condensation was observed in neurons of 30-day-old rats exposed to PA for 19 minutes (Fig. 2). We also observed neurons with dark cytoplasm and vacuoles. Nucleus condensation and compaction, with a festoon shape and twisted nuclear envelope are typical characteristic of neurodegeneration. By morphology these neurons correspond with the Gabaergic Golgi type I neurons.<sup>13,17,19</sup>

### Analysis of striatal GABAergic neuronal loss

Since Gabaergic neurons are the principal target of anoxia, we focused our study only on this type of neurons.<sup>13,20</sup> To quantify the loss of neurons in striatum we employed stereology combined with calbindin immunostaining that identified GABAergic neurons in neostriatum.<sup>13,24</sup> Statistical analysis showed a decreased of the means of calbindin IR neurons that reached statistical significance at 19 minutes of PA ( $P < 0.01$ ) with respect to control group and the rest of the mild PA groups (Table 1).

### Modification in striatal PSDs stained with E-PTA in 1-month-old rat

We did not observe clear alterations in the membranes of dendrites shafts, spines, and neurons were seen in the neostriatal material stained with osmium-lead-citrate in the control and in PA animals (Fig. 3). Ultrastructural organization of pre-synaptic terminals,

3

4

5

6

7

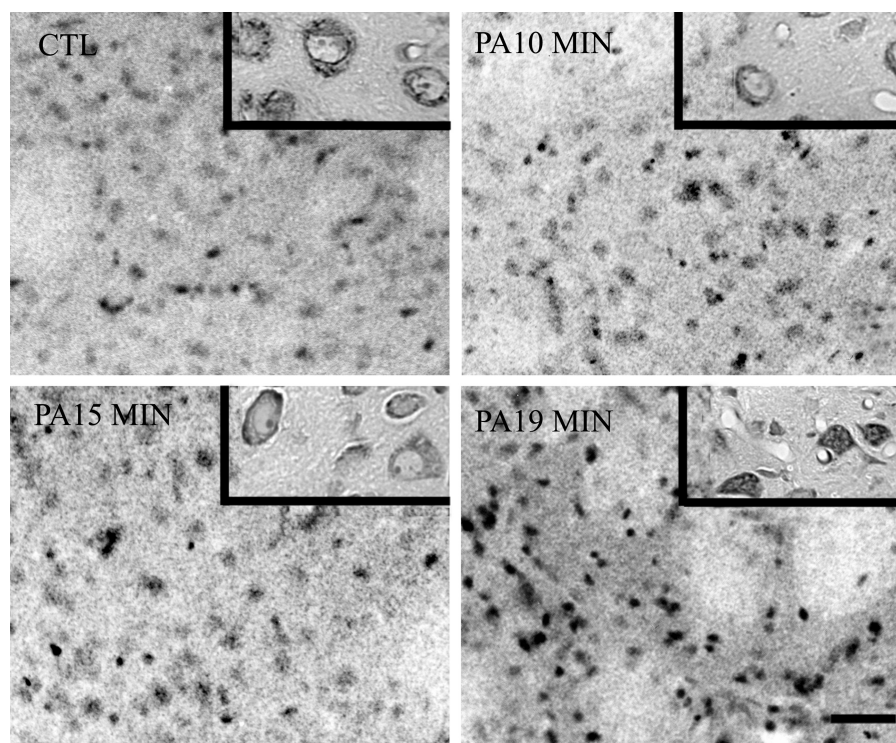


**Figure 1** Low-power micrographs of dorsal neostriatum in 1-month-old rats from control different times of PA Vibratome sections of 50  $\mu\text{m}$  were cut and stained with cresyl violet. A frank neuronal death was observed after 19 minutes (see neurons in the inset). Scale bar, 30  $\mu\text{m}$ .

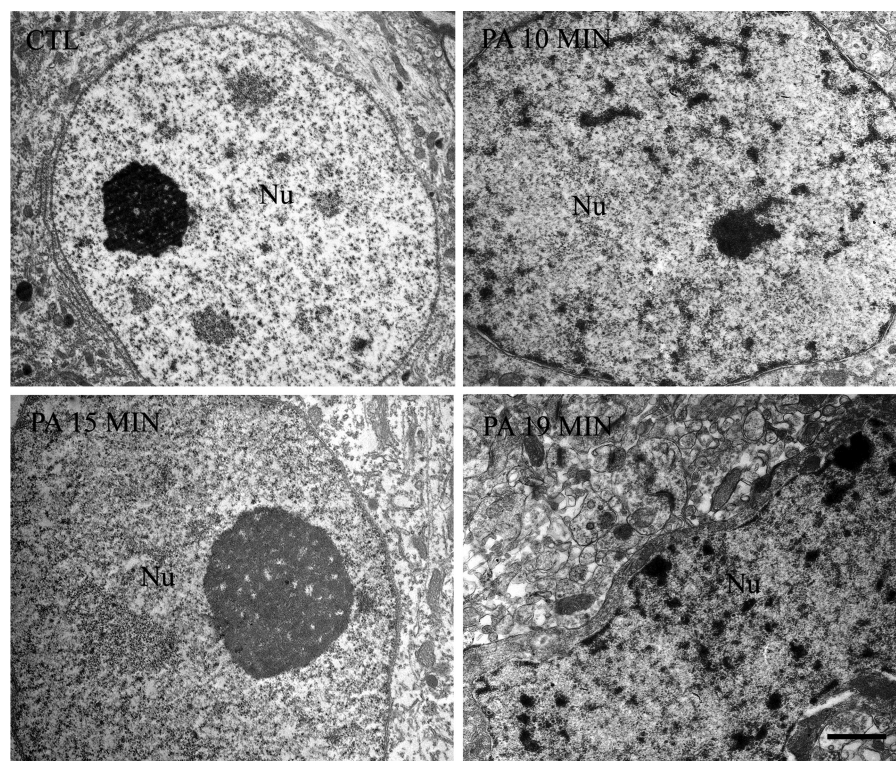


**Figure 2** Electron micrographs of osmium-uranium-lead-stained synapses in dorsal neostriatum from 1-month-old control rats and rats subjected to different times of PA. The synapses (arrows) were intact, and no obvious alterations were seen in these osmium-uranium-lead-stained synapses after PA. AT, axon terminal; DEN, dendritic shaft. Scale bar, 0.5  $\mu\text{m}$ .

pre-synaptic vesicles, and PSDs were intact (Fig. 3). These observations are in agreement with previous ultrastructural studies.<sup>13,16,26-28</sup>

In contrast with the material stained with conventional technique, some alterations were apparent in severe PA in the material stained with E-PTA

**Table 1** Quantification of calbindin positive cell in neostriatum

Groups	Means calbindin IR neurons	Cell loss (%)
Control	702.32 ± 89.39	–
PA 10 minutes	642.11 ± 85.26	–8.54
PA 15 minutes	645.10 ± 119.5	–8.11
PA 19 minutes	558.23 ± 105.6*	–20.51

Data are expressed as means ± SD. Each experimental group was compared to the control group (see text for statistical details). \* $P < 0.05$ .

(Fig. 4). This is consistent with previous studies of other laboratories using a rat model of ischemia<sup>16,27</sup> and our laboratory but in long-term studies.<sup>13</sup> After severe PA, post-asphyctic PSDs were thicker than those observed in controls (Fig. 4). To confirm these changes we conducted a series of quantitative analysis at PSDs at different time points of PA. Significant differences were found in both the minimum and maximum thickness between the control and 19 minutes of PA. No differences between the control and other times of PA were observed (Fig. 4, Table 2).

#### Ubiquitin-protein conjugates in striatal PSDs: western blot analysis

Since E-PTA-stained aggregates could be composed of abnormal protein<sup>13,16,27</sup> and that ubi-protein are commonly present in protein aggregates in neurodegenerative diseases<sup>29</sup> we use western blot to study the ubiquitination level in young PA rats. The isolated PSDs fractions were analyzed by immunoblotting with ubiquitin antibody and quantified (Fig. 5). Ubi-proteins were hardly detected in control and

mild PA animals but clearly increased in severe PA animals.

#### Discussion

In this study, we demonstrated that in striatum of 1-month-old severe post-asphyctic animals, PSDs showed a consistent change in the thickness. These alterations at PSDs level were correlated with ubiquitination level suggesting that post-synaptic structures are one of the major targets for protein ubiquitination in young severe PA rats. Since ubiquitin mainly tags damaged or unfolded proteins, ubiquitination should be related with early protein damage increment in the severe hypoxic animals.

#### Long-term protein ubiquitination in neostriatum after PA

Consistent with other studies in different model of ischemia<sup>17,26–28,30</sup> and using this PA model but in long-term studies<sup>13</sup> we did not observe any alterations in the subcellular organization of ostriatum in material stained with osmium-heavy metals. However, we observed a marked increase in E-PTA-stained material in the severe PA. Since the cortical-striatal afferent represents the 80% of the synapses in the neostriatum and they are asymmetric as we observed using E-PTA staining, our results suggest that at least this class of synapse is affected. These data are consistent with previous observations in hippocampal and neocortical post-ischemic synapses<sup>27</sup> and in our long-term study in PA.<sup>13</sup> We did not analyze whether other synapses were also affected. This question is currently under analysis because dopaminergic synapses are almost

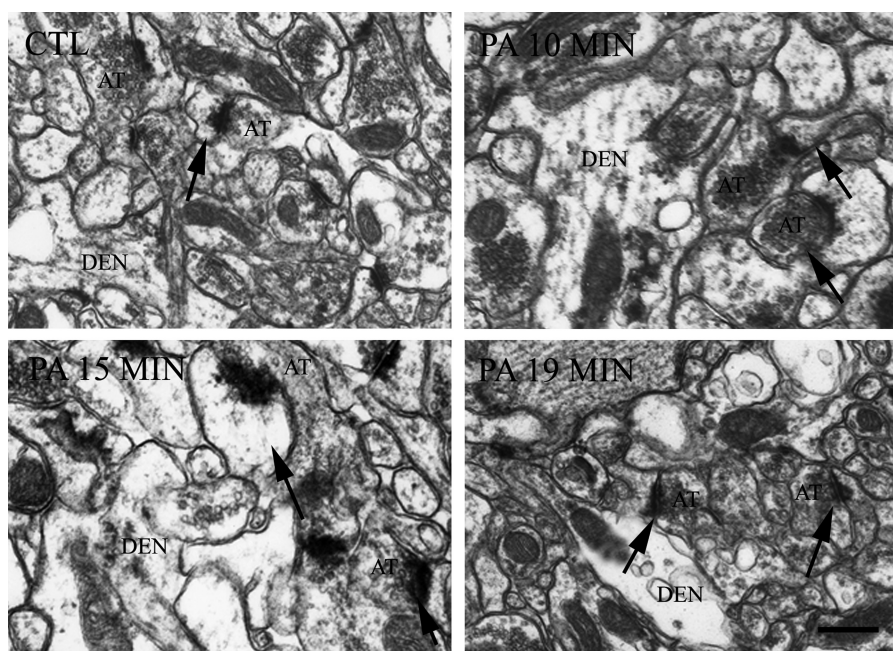


**Figure 3** Electron micrograph of the Golgi Type I neuron (GABAergic neuron) in the neostriatum area from 1-month-old CTL rats and animals subjected to different time of PA. Observe that the morphological characteristics of neurodegeneration in the 19 minutes PA rats are pronounced. Nu, nucleus. Scale bar, 1  $\mu$ m.

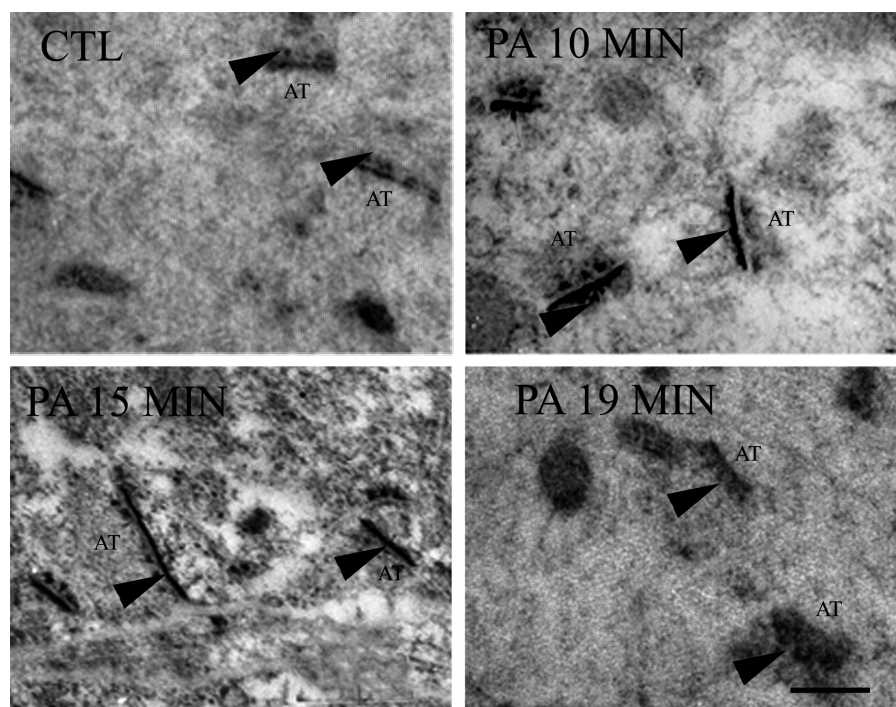


**Figure 4** Electron micrographs of E-PTA stained PSDs (arrowheads) in neostriatal tissue section from 1-month-old rats subjected to different time of PA and control. Note the increased thickness of the PSDs in the severe asphyctic neostriatum, compared with the control and the mild asphyxia. AT, axon terminal. Scale bar, 0.5  $\mu$ m.

**Table 2** Analysis of PSDs features in neostriatum of control, PA groups

Groups	Area $\times 10^3$ (nm <sup>2</sup> )	Length (nm)	Minimum thickness (nm)	Maximum thickness (nm)
Control	2.2 $\pm$ 0.1	92.1 $\pm$ 2.3	15.2 $\pm$ 0.5	42.0 $\pm$ 2.5
10 minutes	3.3 $\pm$ 1.0	99.1 $\pm$ 2.3	24.2 $\pm$ 0.4	55.7 $\pm$ 2.6
15 minutes	3.4 $\pm$ 0.9	99.3 $\pm$ 6.9	24.6 $\pm$ 0.5	55.0 $\pm$ 4.3
19 minutes	5.5 $\pm$ 1.2**	103.1 $\pm$ 5.2	32.6 $\pm$ 0.4**	79.1 $\pm$ 2.2**

Data are expressed as means  $\pm$  SD. Each experimental group was compared to the control group (see text for statistical details). \*\* $P < 0.01$ .

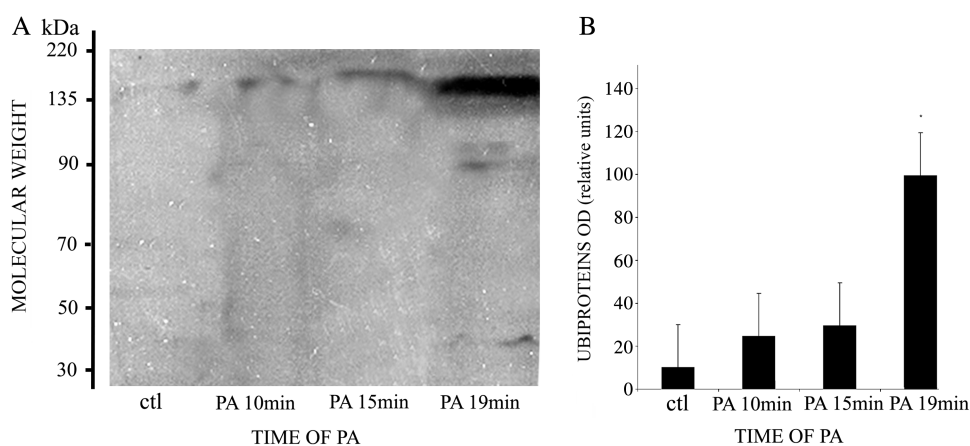


**Figure 5** (A) Immunoblots of ubi-proteins in neostriatal PSDs from 1-month-old rats. PSDs were prepared from control and different time of PA. The blots were labeled with the anti-ubi-protein antibody and visualized with ECL system. Molecular size is indicated at the left. Ubi-proteins are present after PA. HYP 20 prevented the ubi-proteins formation. A mouse anti-actin monoclonal antibody was used as an internal loading control. (B) Quantification of ubi-proteins on PSD. Mean optical intensities of immunoblot bands are expressed as mean  $\pm$  SD. \* $P < 0.01$  between control, hypothermia and hypoxia conditions.

20% of the total synapses in neostriatum. Furthermore, dopamine has been suggested to be one of the neurotransmitter that could be toxic if it is over-release during an ischemic-hypoxic episode.<sup>31</sup>

In contrast with our observation at 6 months, we did not observe increment in the PSDs thickness after 10 and 15 minutes of PA. This could be related to the fact that the cell death in these PA animals was not

significant and probably many proteins of the PSDs were recovered. Analysis using immunoblot for ubiquitin in purified PSDs showed an increase in ubiquitination level in the severe PA PSDs. Although not too much data are available about the mechanism of cell death during PA<sup>13,24</sup> these findings suggest that the increased in the thickness could be related with the degradation of abnormal proteins probably before neurons trigger death mechanisms. Therefore, we think that PSDs send some early signals that could induce long-term neuronal alterations.

### *Significance of the ubiquitin-conjugated protein accumulation as a possible cause of long-term neural damage*

The role of the early ubi-conjugated proteins that we observed in the PSDs of the post-asphyctic is still not clear. However, some data suggest that accumulation of ubi-proteins could be one of the mechanisms involved not only in short-term but also in long-term cell death during PA as we observed in previous reports.<sup>13</sup> Consistent with this view, persistent ubiquitination was found in the hippocampal neurons PSDs<sup>16,32</sup> after transient cerebral ischemia<sup>17</sup> suggesting that increased ubi-protein conjugates might produce protein damage. Because the GABAergic neurons received most of the glutamatergic input, these alterations might result in a toxic signal, such as a greater calcium influx propagating to the dendritic shaft and the cell body, that finally cause cell degeneration as we extensively describe in different reports.<sup>10</sup> In addition, the increment in the calcium levels, mediated calpain activation and ROS production after hypoxic-ischemic insult is able to damage proteins.<sup>8,9,33,34</sup> Ischemic acidosis may contribute to ubiquitin conjugates accumulation because protein folding is pH-dependent.<sup>35</sup> On the other hand, induction of heat shock proteins (HSPs) protects the neuron against ischemic insults.<sup>36,37</sup> Hu *et al.*<sup>26</sup> has reported translocation of both HSC 70 and NSF into PSDs after ischemia, destined to prevent protein misfolding. Since degradation of ubi-proteins requires the presence of molecular chaperones<sup>38</sup> the no proper functioning of this system could finally finish in PSD damage by ubi-protein accumulation. While other HSPs reversibly attach to denatured proteins and help to refold or reassemble them, the ubiquitin-conjugated proteins are degraded by 26S proteasome.<sup>29</sup> If PA insult is not removed in time from the cell, the ubiquitin pathway that is working in excess, might affect the neuronal survival, since neurons does not have the capacity to remove damage proteins, thus they are accumulated. Finally, accumulation of ubi-proteins leads the neurons to death.

Since striatum is rich in spines and the spines are structures highly F-actin concentrated actin<sup>33</sup> could

be one of the proteins affected. Some studies *in vitro* showed alteration in the depolymerization–repolymerization cycle in dendritic spines during ischemia.<sup>39</sup> We also observed similar alterations after 1 month of PA. Some preliminary results were published in Capani *et al.*<sup>40</sup>

Finally, overproduction of ubiquitin-conjugated proteins can produce dysfunctional synaptic transmission. Physiological study in neostriatum<sup>41</sup> has demonstrated that the evoked post-synaptic responses of spiny neurons are suppressed and the excitability of spiny neurons is decreased after transient ischemia. Alterations in the synaptic transmission have been reported during the post-ischemic phase in other areas.<sup>41</sup>

### Conclusions

Overall our data suggest that an excessive protein-ubiquitination in striatal PSDs of 1 month severe PA seems to be related with the increment in the PSD protein accumulation. Although further studies will be necessary to determine the role of this early accumulation of ubi-protein in the PDS, it is tempting to speculate that PSDs alterations might be involved in the generation of an aberrant biochemical pathway that lead in long-term modifications in the brain of the PA animals as we describe in previous paper.<sup>13</sup> In agreement with this point of view, Alzheimer disease has a deleterious action on actin cytoskeleton linked with PSDs, leading to dendritic spines dysfunction and synaptic degeneration.<sup>42</sup>

### Acknowledgments

This work was supported by Kennedy University Research Grant.

### References

- 1 Younkin DP. Hypoxic-ischemic brain injury of the newborn—statement of the problem and overview. *Brain Pathol* 1992;2: 209–10.
- 2 Pulsinelli WA. Selective neuronal vulnerability: morphological and molecular characteristics. *Prog Brain Res* 1985;63:9–37.
- 3 Wieloch T, Miyauchi Y, Lindvall O. Neuronal damage in the striatum following forebrain ischemia: lack of effect of selective lesions of mesostriatal dopamine neurons. *Exp Brain Res* 1990; 83:159–63.
- 4 Hill A, Volpe JJ. Seizures hypoxic-ischemic brain injury and intraventricular hemorrhage in the newborn. *Ann Neurol* 1991; 10:109–21.
- 5 Osborne NN, Casson RJ, Wood JP, Chidlow G, Graham M, Melena J. Retinal ischemia: mechanisms of damage and potential therapeutic strategies. *Prog Retin Eye Res* 2004;23:91–147.
- 6 Shankaran S. Neonatal encephalopathy: treatment with hypothermia. *J Neurotrauma* 2009;26:437–43.
- 7 Vannucci RC, Perlman JM. Interventions for perinatal hypoxic-ischemic encephalopathy. *Pediatrics* 1997;100:1004–14.
- 8 Capani F, Loidl CF, Aguirre F, Piehl L, Facorro G, Hager A, *et al.* Changes in reactive oxygen species (ROS) production in rat brain during global perinatal asphyxia: an ESR study. *Brain Res* 2001;914:204–7.
- 9 Capani F, Loidl CF, Piehl L, Facorro G, De Paoli T, Hager A. Long term production reactive oxygen species during perinatal asphyxia in the rat central nervous system: effects of hypothermia. *Int J Neurosci* 2003;113:641–54.

- 10 Choi DW. Calcium: still center-stage in hypoxic-ischemic neuronal death. *Trend Neurosci* 1995;18:58–60.
- 11 Herrera-Marschitz M, Loidl CF, You ZB, Andersson K, Silveira R, O'Connor WT, *et al.* Neurocircuitry of the basal ganglia studied by monitoring neurotransmitter release. Effect of intracerebral and perinatal asphyxia lesions. *Mol Neurobiol* 1994;9:171–82.
- 12 Aon-Bertolino ML, Romero JI, Galeano P, Holubiec M, Badorrey MS, Saraceno GE, *et al.* Thioredoxin and glutaredoxin system proteins-immunolocalization in the rat central nervous system. *Biochim Biophys Acta* 2011;1810:93–110.
- 13 Capani F, Saraceno GE, Botti V, Aon-Bertolino L, de Oliveira DM, Barreto G, *et al.* Protein ubiquitination in postsynaptic densities after hypoxia in rat neostriatum is blocked by hypothermia. *Exp Neurol* 2009;219(2):404–13.
- 14 Kirino T, Tamura A, Sano K. Delayed neuronal death in the rat hippocampus following transient forebrain ischemia. *Acta Neuropathol* 1984;64:139–47.
- 15 Van de Berg WD, Schmitz C, Steinbusch HW, Blanco CE. Perinatal asphyxia induced neuronal loss by apoptosis in the neonatal rat striatum: a combined TUNEL and stereological study. *Exp Neurol* 2002;174:29–36.
- 16 Hu BR, Martone ME, Jones YZ, Liu CL. Protein aggregation after transient cerebral ischemia. *J Neurosci* 2000;20:3191–9.
- 17 Liu CL, Ge P, Zhang F, Hu BR. Protein ubiquitination in postsynaptic densities after transient cerebral ischemia. *J Cereb Blood Flow Metab* 2004;24:1219–25.
- 18 Mengesdorf T, Jensen PH, Mies G, Aufenberg C, Paschen W. Down regulation of parkin protein in transient focal cerebral ischemia: a link between stroke and degenerative disease?. *Proc Natl Acad Sci USA* 2002;99:15042–7.
- 19 Capani F, Loidl CF, López-Costa JJ, Pecci Saavedra J. Ultrastructural changes in NOS immunoreactivity in rat brain during perinatal asphyxia: neuroprotective effects of hypothermia. *Brain Res* 1997;775:11–23.
- 20 Galeano P, Blanco Calvo E, Madureira de Oliveira D, Cuenya L, Kamenetzky GV, Mustaca AE, *et al.* Long-lasting effects of perinatal asphyxia on exploration, memory and incentive downshift. *Int J Dev Neurosci* 2011 May 27. [Epub ahead of print].
- 21 Loidl CF, Gavilanes AW, Van Dijk EH, Vreuls W, Blokland A, Vles JS, *et al.* Effects of hypothermia and gender on survival and behavior after perinatal asphyxia in rats. *Physiol Behav* 2000;68:263–9.
- 22 Fiala JC, Feinberg M, Popov V, Harris KM. Synaptogenesis via dendritic filopodia in developing hippocampal area CA1. *J Neurosci* 1998;18:8900–11.
- 23 Dorfman VB, Vega MC, Coirini H. Age-related changes of the GABA-B receptor in the lumbar spinal cord of male rats and penile erection. *Life Sci* 2006;78:1529–34.
- 24 Van de Berg WD, Kwajitall M, de Louw AJ, Lissone NP, Schmitz C, Faull RL, *et al.* Impact of perinatal asphyxia on the GABAergic and locomotor system. *Neuroscience* 2003;117:83–96.
- 25 Hu BR, Wieloch T. Tyrosine phosphorylation and activation of mitogen-activated protein kinase in the rat brain following transient cerebral ischemia. *J Neurochem* 1994;62:1357–67.
- 26 Hu BR, Park M, Martone ME, Fischer WH, Ellisman MH, Zivin JA. Assembly of proteins to postsynaptic densities after transient cerebral ischemia. *J Neurosci* 1998;18:625–33.
- 27 Martone ME, Jones YZ, Young SJ, Ellisman MH, Zivin JA, Hu BR. Modification of postsynaptic density after transient cerebral ischemia: a quantitative and three-dimensional ultrastructural study. *J Neurosci* 1999;15:1988–97.
- 28 Petito CK, Pulsinelli WA. Sequential development of reversible and irreversible neuronal damage following cerebral ischemia. *Exp Neurol* 1984;43:141–53.
- 29 Korhonen L, Lindholm D. The ubiquitin proteasome system in synaptic and axonal: a new twist to an old cycle. *J Cell Biol* 2004;165:27–30.
- 30 Petito CK, Pulsinelli WA, Jacobson G, Plum F. Edema and vascular permeability in cerebral ischemia: comparison between neuronal damage and infarction. *J Neuropath Exp Neurol* 1982;4:423–36.
- 31 Nishino H, Hida H, Kumazaki M, Shimano Y, Nakajima K, Shimizu H, *et al.* The striatum is the most vulnerable region in the brain to mitochondrial energy compromise: a hypothesis to explain its specific vulnerability. *J Neurotrauma* 2000;17:251–60.
- 32 Liu JJ, Zhao H, Sung JH, Sun GH, Steinberg GK. Hypothermia blocks ischemic changes in ubiquitin distribution and levels following stroke. *Neuroreport* 2006;17:1691–5.
- 33 Capani F, Martone ME, Deerinck TJ, Ellisman MH. Selective localization of high concentrations of F-actin in subpopulations of dendritic spines in rat central nervous system: a three-dimensional electron microscopic study. *J Comp Neurol* 2001;435:156–70.
- 34 Dingman A, Lee SY, Darugin N, Wendland MF, Vexler S. Aminoguanidine inhibits caspase-3 and calpain activation without affecting microglial activation following neonatal transient cerebral ischemia. *J Neurochem* 2006;96:1467–79.
- 35 Kraig RP, Wagner RJ. Acid-induced changes of brain protein buffering. *Brain Res* 1987;410:390–4.
- 36 Sharp FR, Massa SM, Swanson RA. Heat-shock protein protections. *Trends Neurosci* 1999;22:97–9.
- 37 Yenari MA, Fink SL, Sun GH, Chang LK, Patel MK, Kunis DM, *et al.* Gene therapy with HSP72 is neuroprotective in rat models of stroke and epilepsy. *Ann Neurol* 1998;44:584–91.
- 38 Imai J, Yashiroda H, Maruya M, Yahara I, Tanaka K. Proteasomes and molecular chaperones: cellular machinery responsible for folding and destruction of unfolded proteins. *Cell Cycle* 2000;2:585–90.
- 39 Gisselsson LL, Matus A, Wieloch T. Actin redistribution underlies the sparing effect of mild hypothermia on dendritic spine morphology after *in vitro* ischemia. *J Cereb Blood Flow Metab* 2010;25:1346–55.
- 40 Capani F, Saraceno E, Boti VR, Aon-Bertolino L, Fernández JC, Gato F, *et al.* A tridimensional view of the organization of actin filaments in the central nervous system by use of fluorescent photooxidation. *Biocell* 2008;32(1):1–8.
- 41 Xu ZC. Neuropsychological changes of spiny neurons in rat neostriatum after transient forebrain ischemia: an *in vivo* intracellular recording and staining study. *Neuroscience* 1995;67:823–36.
- 42 Penzes P, Vanleeuwen JE. Impaired regulation of synaptic actin cytoskeleton in Alzheimer's disease. *Brain Res Rev* 2011;67:184–92.
- 43 Bjelke B, Andersson K, Ögren SO, Bolme P. Asphyctic lesion: proliferation of tyrosine hydroxylase-immunoreactive nerve cell bodies in the rat substantia nigra and functional changes in dopamine neurotransmission. *Brain Res* 2004;543:1–9.

10

11



# Authors Queries

Journal: **Nutritional Neuroscience**

Paper: **NNS81**

Article title: **Early changes in the synapses of the neostriatum induced by perinatal asphyxia**

Dear Author

During the preparation of your manuscript for publication, the questions listed below have arisen.

Please attend to these matters and return this form with your proof. Many thanks for your assistance

<b>Query Reference</b>	<b>Query</b>	<b>Remarks</b>
1	Please check and provide the complete corresponding address with postal code.	
2	Please check Amiel-Tison et al., 1986; Gunn et al., 2000 are not cited in reference list. Please cite, else delete from the text.	
3	Please provide the manufacturer location city, state(if USA) and country for Chemicon.	
4	Please provide the full form of RT.	
5	Please provide the full form of ECL.	
6	Please provide the manufacturer location city, state(if USA) and country for Amersham.	
7	Please provide the full form of IR.	
8	Please provide the full form of CTL.	
9	Please provide the full form of NSF.	
10	Please provide the volume and page numbers for reference 20.	
11	Ref. 43 is not cited in the text. Please cite else delete from the list.	